BIOLOGY OF REPRODUCTION (2014) **90**(3):48, 1–11
Published online before print 22 January 2014.
DOI 10.1095/biolreprod.113.113118

Loss of Sertoli-Germ Cell Adhesion Determines the Rapid Germ Cell Elimination During the Seasonal Regression of the Seminiferous Epithelium of the Large Hairy Armadillo *Chaetophractus villosus*[1]

Juan Pablo Luaces,[5] Luis Francisco Rossi,[5] Roberta Beatriz Sciurano,[5] Paola Rebuzzini,[6] Valeria Merico,[6] Maurizio Zuccotti,[4,7] Maria Susana Merani,[3,5] and Silvia Garagna[2,6,8]

[5]*Laboratorio de Biología Cromosómica, Facultad de Medicina, Universidad de Buenos Aires, Buenos Aires, Argentina*
[6]*Laboratorio di Biologia dello Sviluppo, Dipartimento di Biologia e Biotecnologie "Lazzaro Spallanzani," Università degli Studi di Pavia, Pavia, Italy*
[7]*Dipartimento di Scienze Biomediche, Biotecnologiche e Traslazionali (S.Bi.Bi.T.), Sezione di Anatomia, Istologia ed Embriologia, University of Parma, Parma, Italy*
[8]*Centro di Ingegneria Tissutale, Università degli Studi di Pavia, Pavia, Italy*

ABSTRACT

The armadillo *Chaetophractus villosus* is a seasonal breeder whose seminiferous epithelium undergoes rapid regression with massive germ cell loss, leaving the tubules with only Sertoli cells and spermatogonia. Here, we addressed the question of whether this regression entails 1) the disassembly of cell junctions (immunolocalization of nectin-3, Cadm1, N-cadherin, and beta-catenin, and transmission electron microscopy [TEM]); 2) apoptosis (immunolocalization of cytochrome *c* and caspase 3; TUNEL assay); and 3) the involvement of Sertoli cells in germ cell phagocytosis (TEM). We showed a dramatic reduction in the extension of vimentin filaments associated with desmosomelike junctions at the interface between Sertoli and germ cells, and an increased diffusion of the immunosignals of nectin-3, Cadm1, N-cadherin, and beta-catenin. Together, these results suggest loss of Sertoli-germ cell adhesion, which in turn might determine postmeiotic cell sloughing at the beginning of epithelium regression. Then, loss of Sertoli-germ cell adhesion triggers cell death. Cytochrome *c* is released from mitochondria, but although postmeiotic cells were negative for late apoptotic markers, at advanced regression spermatocytes were positive for all apoptotic markers. Transmission electron microscopy analysis showed cytoplasmic engulfment of cell debris and lipid droplets within Sertoli cells, a sign of their phagocytic activity, which contributes to the elimination of the residual meiocytes still present in the latest regression phases. These findings are novel and add new players to the mechanisms of seminiferous epithelium regression occurring in seasonal breeders, and they introduce the armadillo as an interesting model for studying seasonal spermatogenesis.

adhesion molecules, anoikis, apoptosis, Cadm1, intermediate filaments, N-cadherin and β-catenin, nectin-3, phagocytosis, seasonal reproduction, spermatogenesis, testosterone

INTRODUCTION

The large hairy armadillo, *Chaetophractus villosus* (superorder Xenarthra, Cope, 1889) is one of the most common species of armadillo in Argentina [1], where it is present in large populations, indicative of successful reproductive strategies, including seasonal reproduction [2, 3]. In males, this seasonal reproduction entails a period of spermatogenesis inactivity. In animals captured from the beginning of winter (July-August) until the end of summer-beginning of autumn (March-early April), the seminiferous epithelium is made of eight stages of cellular associations at different steps of differentiation, a histologic organization indicative of an active spermatogenesis [3]. In males captured between mid-April and June (mid-autumn-end of autumn), a regression of the seminiferous epithelium, which occurs through massive detachment of meiotic and postmeiotic cells, suddenly leads to the sole presence of Sertoli cells and spermatogonia, a sign of inactivity of the spermatogenic process during this period of the year [3].

The sequence of events, the cellular process, and the molecular players that lead to this rapid regression are as yet unknown. Apoptosis has been described as playing an important role in the process of regression of the seminiferous epithelium in several seasonal breeders, such as hamsters [4, 5], white-footed mice [6], and the European brown hare [7]. Instead, in other species, like the roe deer [8] and the Iberian mole *Talpa occidentalis* [9], apoptosis does not appear to be the principal cause. Indeed, in the Iberian mole, the absence of cells positive to the late apoptotic TUNEL marker led Dadhich et al. [10] to describe a phenomenon of live germ cell desquamation, regulated by the modulation of the expression and distribution of cell-to-cell adhesion molecules, as a major mechanism of seasonal testis regression. Importantly, in both the large hairy armadillo [3] and the Iberian mole [10], the cell shedding observed coincides with low testosterone levels in the testis.

[1]Supported by the University of Pavia (Fondo di Ateneo per la Ricerca). M.S.M. acknowledges support from the Agencia Nacional de Promoción Científica y Tecnológica (PICT 1198), Argentina; and the Consejo Nacional de Investigaciones Científicas y Técnicas (PIP 0204), Argentina.
[2]Correspondence: Silvia Garagna, Laboratorio di Biologia dello Sviluppo, Dipartimento di Biologia e Biotecnologie "Lazzaro Spallanzani", Università degli Studi di Pavia, Via Ferrata 9, 27100 Pavia, Italy. E-mail: silvia.garagna@unipv.it
[3]Correspondence: Maria Susana Merani, Laboratorio de Biología Cromosómica, Facultad de Medicina, UBA, Paraguay 2155 10°P Lab 6, Buenos Aires, Argentina. E-mail: mmerani@fmed.uba.ar
[4]Correspondence: Maurizio Zuccotti, Dipartimento di Scienze Biomediche, Biotecnologiche e Traslazionali (S.Bi.Bi.T.), Sezione di Anatomia, Istologia ed Embriologia, University of Parma, Parma 43100, Italy. E-mail: maurizio.zuccotti@unipr.it

Received: 13 August 2013.
First decision: 9 September 2013.
Accepted: 14 January 2014.

eISSN: 1529-7268 http://www.biolreprod.org
ISSN: 0006-3363

TABLE 1. Animal identification numbers, testis activity based on the histological classification of the status of the seminiferous epithelium, and type of analysis performed for each individual.

Identification no.	Phase of testis activity	Cyt-C	Caspase 3	TUNEL	Nectin-3	Cadm1	N-cadherin	β-catenin	TEM
1024-1	Active	X	X	X	–	–	–	–	X
1026-1	Active	X	X	X	X	X	X	X	X
1044	Active	X	X	X	X	X	X	X	–
1060	Active	X	X	X	X	X	X	X	–
1060-1	Active	X	X	X	X	X	X	X	–
1050-3	I	X	X	X	X	X	X	X	–
1051-1	I	X	X	X	X	X	X	X	–
1051-3	I	X	X	X	X	X	X	X	–
960	II	X	X	X	X	X	X	X	–
1050-1	III	X	X	X	X	X	X	X	–
1055-1	III	X	X	X	X	X	X	X	X
1055-3	III	X	X	X	X	X	X	X	X
1057	III	X	X	X	–	–	–	–	–
1014-3	IV	X	X	X	X	X	X	X	–
1014-5	IV	X	X	X	X	X	X	X	X
1014-1	IV	X	X	X	X	X	X	X	–

In the present study, we addressed the question of whether the regression of the seminiferous epithelium of *C. villosus* involves 1) the disassembly of cell junctions (by the immunolocalization of nectin-3, cell adhesion molecule-1 [Cadm1], N-cadherin adhesion molecules, and β-catenin; and, by transmission electron microscopy [TEM], the intercellular junctions) and 2) apoptotic events (by the immunolocalization of cytochrome *c* and caspase 3, and the TUNEL assay), or whether it is rather a phenomenon of live germ cell desquamation. Also, by TEM we studied the involvement of Sertoli cells in the process of germ cell detachment and phagocytosis.

MATERIALS AND METHODS

Samples

Testes from 16 animals [3], fixed either in 10% formalin or in Bouin fluid, were selected from a collection of specimens captured in the area of Loma Verde (35°16′S; 58°23′W; http://g.co/maps/sswm), Province of Buenos Aires, Argentina, during 2005–2012 (permission N. 22300, Ministerio de Asuntos Agrarios y Producción, Departamento de los Recursos Naturales, Provincia de Buenos Aires). In Table 1, the samples, chosen on the basis of the state of activity of their seminiferous epithelium (Luaces et al. [3] and Luaces, unpublished results), and the type of analysis performed are reported.

For the analysis of apoptosis, two 5-μm transverse cross-testis sections were mounted onto each of four slides of a histological series. For each testis, this series was repeated twice. One slide was stained with the periodic acid-Schiff (PAS) reaction and counterstained with hematoxylin; the other three were kept for subsequent assays. Likewise, the same protocol was used for the study of cell junction disassembly.

Immunohistochemical Analysis

Following deparaffinization and rehydration, slides were used to separately reveal cytochrome *c* and caspase 3 apoptotic markers and the adhesion molecules nectin-3, Cadm1, N-cadherin, and β-catenin. Antigen retrieval was carried out in 10 mM sodium citrate (Sigma) and 0.05% Tween 20 (product no. P9416; Sigma), pH 6.0 [11]. Then, to prevent nonspecific binding of the primary antibody, sections were incubated with 1% v/v fetal bovine serum (product no. 10270-106; Invitrogen) in PBS (137 mM NaCl, 2.7 mM KCl, 10 mM Na_2HPO_4, and 2 mM KH_2PO_4; Sigma)—with the exception of slides used for N-cadherin, in which 4% v/v fetal bovine serum in PBS was used—for 10 min. On separate slides, the following primary antibodies were applied at a dilution of 1:100 in PBS with 1% v/v fetal bovine serum—with the exception of N-cadherin, in which 4% v/v fetal bovine serum in PBS was used—at 37°C for 1 h: rabbit anti-mouse nectin-3, Cadm1, N-cadherin, or β-catenin polyclonal antibodies (product nos. ab 63931, ab3910, ab 12221, and ab 32572, respectively; Abcam). Rabbit anti-mouse caspase 3 polyclonal antibody (product no. 9661; Cell Signaling Technology) was used at a dilution of 1:100 in PBS with 1% w/v bovine serum albumin (product no. A3311; Sigma) at 4°C overnight. After three washes in PBS, sections were incubated with anti-rabbit secondary Cy3-conjugated antibody diluted in PBS for 30 min at room temperature, washed again, counterstained with 0.1 μg/ml 4′,6′-diaminido-2-phenylindole, and mounted in VECTASHIELD Mounting Medium antifading (product no. H-1000; Vector Laboratories).

Cytochrome *c* was detected using an indirect immunoperoxidase method. Sections were incubated for 15 min in 0.5% v/v H_2O_2 diluted in methanol to block endogenous peroxidase activity, rinsed in PBS, and incubated with a solution of 1% w/v bovine serum albumin in PBS for 10 min to prevent nonspecific binding of the primary antibody. Purified mouse anti-mouse cytochrome *c* monoclonal antibody (product no. 556433; BD Pharmingen) was used at a dilution of 1:500 in PBS at 37°C for 1 h. After three washes in PBS, sections were incubated with secondary peroxidase-conjugated antibodies diluted in PBS for 30 min and developed with 3,3′-diaminobenzidine (DAB; product no. D3939; Sigma). Methyl green (0.5% w/v for 10 min at room temperature) was used as a counterstain. In negative controls, primary antibodies were omitted.

TUNEL Assay

For the evaluation of late apoptotic events, an ApopTag Plus Peroxidase In Situ Apoptosis Kit (product no. S7101; Chemicon-Millipore) was used following the manufacturer's instructions. Permeabilization was carried out with proteinase K (20 mg/ml) for 10 min. Sections were then treated for 5 min to 3% v/v H_2O_2 to reduce the activity of endogenous peroxidase, incubated with the terminal deoxynucleotidyl transferase (TdT) labeling reaction mix for 1 h at 37°C, washed in PBS, incubated with antidigoxigenin, and finally developed with DAB. Positive control slides contained in the same kit were processed as stated in the manufacturer's instructions. For negative controls, sections were processed without TdT enzyme in the labeling reaction mix. Methyl green (0.5% w/v for 10 min at room temperature) was used to counterstain the sections.

Slides processed for immunohistochemical analysis and the TUNEL assay were examined with an Olympus BX60 fluorescence microscope; images were captured with a DP72 camera (Olympus) and processed using the cellSens 1.4.1 software (Olympus). For each slide, a minimum of 88 to a maximum of 202 transverse tubule cross sections were analyzed.

Transmission Electron Microscopy

Prior to Bouin fixation, a piece of parenchyma was fixed for TEM in 2.5% glutaraldehyde in 0.1 M cacodylate buffer, pH 6.9, at room temperature for 2 h; then, specimens were postfixed in 1% OsO_4 (product no. 20816-12-0; Polysciences Inc.). Samples were embedded in Araldite (product no. AR502; Sigma-Aldrich). Serial (0.08 μm) sections for TEM were cut in a Porter-Blum ultramicrotome (Sorvall Inc.), picked up in single-hole grids, and stained with a saturated solution of uranyl acetate and lead citrate (0.3%). Micrographs were obtained with a Zeiss EM 109T, equipped with a Gatan ES1000W digital camera, at the LANAIS service from CONICET.

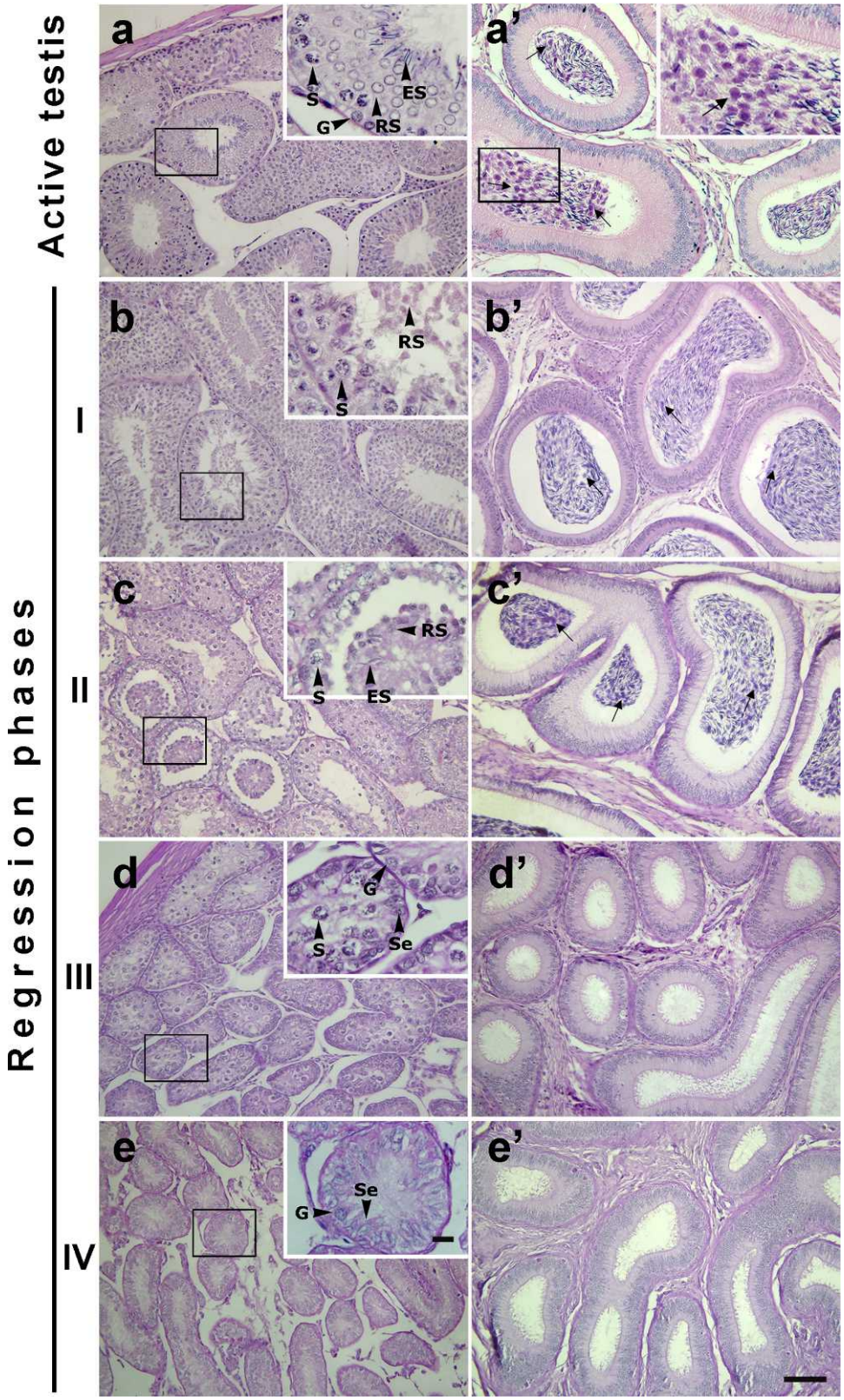

FIG. 1. The seminiferous epithelium of individuals with active spermatogenesis or during the four phases of regression. Histological sections (PAS stained) of testes (**a**–**e**) and epididymides (**a**′–**e**′) of individuals with active (**a** and **a**′) or regressing (**b**–**e** and **b**′–**e**′) spermatogenesis. Se, Sertoli cell; G, spermatogonium; S, spermatocyte; RS, round spermatid; ES, elongated spermatid. In **a**′, **b**′, and **c**′, arrows indicate sperm heads, showing their oval shape. Bar = 100 μm; inset bar = 20 μm.

RESULTS

Regression of the Seminiferous Epithelium Occurs Through Progressive Cell Depletion

In the five animals captured from the beginning of July to the end of March/beginning of April, the seminiferous epithelium was made of Sertoli cells and four/five concentric layers of germ cells at specific and progressive stages of differentiation (Fig. 1a) [3]. In these animals, spermatozoa were present in the lumen of the epididymis (Fig. 1a′). For 11 animals captured during the regression period [3], on a morphological basis we distinguished four main phases of epithelium regression. The seminiferous epithelium of four animals was classified as phase I (Fig. 1b), whereby 70% of tubules presented normal morphology, whereas the remaining 30% showed round spermatids detached from the epithelium and released into the lumen [3]; spermatozoa were still observed into the epididymis (Fig. 1b′). One animal showed advanced regression of the seminiferous epithelium (phase II; Fig. 1c), with the great majority of tubules undergoing massive cell loss of postmeiotic cells, which were released into the lumen. In the epididymis sections, we observed only spermatozoa (Fig. 1c′), some of which appeared with their large, oval, spoonlike shape [12, 13] as a consequence of the section cutting plane. For their morphology, spermatozoa were easily identifiable from immature postmeiotic cells, which were not seen in the sections analyzed. This same sperm morphology was visible also in the epididymis of animals with active testes (Fig. 1a′). After losing postmeiotic cells, animals became completely azoospermic, their seminiferous tubules presenting a disrupted epithelial organization maintaining spermatogonia and few spermatocytes (phase III; Fig. 1d), or, in a further step, only spermatogonia (phase IV; Fig. 1e). The four animals in phase III and the three animals in phase IV, lacking spermatozoa in their epididymis (Fig. 1, d′ and e′), were classified as inactive.

Shedding of Germ Cells Correlates with Diffusion of Molecules Involved in the Adhesion Between Sertoli and Germ Cells

The abrupt massive detachment of cells observed during regression of the seminiferous epithelium suggests a modification of the adhesion junctions between Sertoli and germ cells [10]. To test this hypothesis, we analyzed the immunofluorescence pattern of localization of nectin-3, Cadm1, N-cadherin, and β-catenin in the seminiferous epithelium throughout regression (Fig. 2).

Nectin-3 is a Ca^{2+}-independent immunoglobulin-like cell-cell adhesion molecule. In the mouse it is localized around the head of maturing spermatids and is involved in the maintenance of the anchorage with Sertoli cells until spermiation [14]. In the armadillo seminiferous epithelium, nectin-3 had a localization similar to that in the mouse, with a sharp immunofluorescence signal that clearly surrounded the entire elongating spermatid head (Fig. 2d, arrowheads) and, at later stages of differentiation, became brighter at the tip of the acrosome (Fig. 2d, arrow). At an early stage of seminiferous epithelium regression (phase I; Fig. 2e), the nectin-3 signal blurred, losing its sharpness (Fig. 2e). With the advancement of regression, soon after spermatid detachment, the immunosignal disappeared (Supplemental Fig. S1, available online at www.biolreprod.org) and, at the latest phases, none of the remaining cells had a positive result, likely because of the lack of the nectin-3 protein in both spermatogonia and Sertoli cells (Fig. 2f) [14].

Cadm1 belongs to the spermatogenic immunoglobulin superfamily; in the mouse seminiferous epithelium it is detected in intermediate spermatogonia until the early pachytene spermatocytes and in elongating spermatids, whereas it is absent in round spermatids, mature spermatozoa, and Sertoli cells [15]. In the armadillo active seminiferous tubules, faint Cadm1 immunofluorescence signals were detected in spermatogonia (Fig. 2g, arrow); they were sharp between spermatocytes (Fig. 2g, arrowhead) and surrounded round spermatids and elongating spermatids (Fig. 2g, double arrowhead). At phase I regression, the immunofluorescence pattern remained substantially unchanged, although the signal appeared much more diffused (Fig. 2h). Cadm1 signal was still observable on sloughed spermatids (Supplemental Fig. S1), and when regression of the seminiferous epithelium was almost complete, it was detectable around spermatogonia (Fig. 2i, arrow).

N-cadherin is a calcium-dependent cell-cell adhesion glycoprotein that, in the mouse, is involved as a component, together with E-cadherin and β-catenin of the adherens junctions, in the adhesion between Sertoli cells and spermatocytes and between Sertoli cells and elongated spermatids [16]. In the active seminiferous epithelium of the armadillo, a strong fluorescent continuous dotted signal was observed in the basal compartment surrounding spermatogonia (Fig. 2j, arrow) and was seen with a more rarefied dotted pattern on spermatocytes (Fig. 2j, arrowhead) and on round and elongating spermatids (Fig. 2j, asterisk). In phase I (Fig. 2k) and phase II (Supplemental Fig. S1) regression, the immunofluorescent signal remained localized on the same cell types, albeit with a more dispersed and blurred pattern in spermatocytes (Fig. 2k, arrowhead) and spermatids (Fig. 2k, asterisks). When regression was almost completed (Fig. 2l), the tubule shrinkage did not allow for an accurate description of the localization of the signal around the cells on the basal compartment; instead, a diffused fluorescence towards the lumen likely uncovered the Sertoli cell domains (Fig. 2l, double arrowhead). Of the very few spermatocytes left, those closer to the basal compartment maintained a signal, whereas those present in the lumen were negative (Fig. 2l, arrowhead).

β-Catenin is a crucial molecule that bridges Sertoli-germ cell adhesion and whose signaling cascade is required for postmeiotic germ cell differentiation [17]. In the mouse, β-catenin is found between Sertoli cells and between Sertoli cells and the distal portion of elongating spermatids [17]. In the armadillo (Fig. 2m), a strong fluorescent signal decorated the spermatogonia present in the basal compartment (Fig. 2m, arrow) and also marked both meiotic (Fig. 2m, arrowhead) and postmeiotic (Fig. 2m, double arrowhead) cells. At phase I regression, the signal pattern was maintained around spermatogonia (Fig. 2n, arrow), whereas it was faint and diffuse in meiotic cells, particularly in the sloughed postmeiotic cells (Fig. 2n, arrowhead). The same pattern was observed in phase II (Supplemental Fig. S1). When the epithelium was almost fully regressed, the β-catenin signal was localized around the remaining cells, except for the few spermatocytes still present (Fig. 2o, arrowhead).

Apoptosis Is Involved in Germ Cell Loss During Spermatogenesis Regression

To investigate whether the cells detached from the epithelium and found in the tubule lumen undergo cell death, different markers were assayed. Testis sections were stained

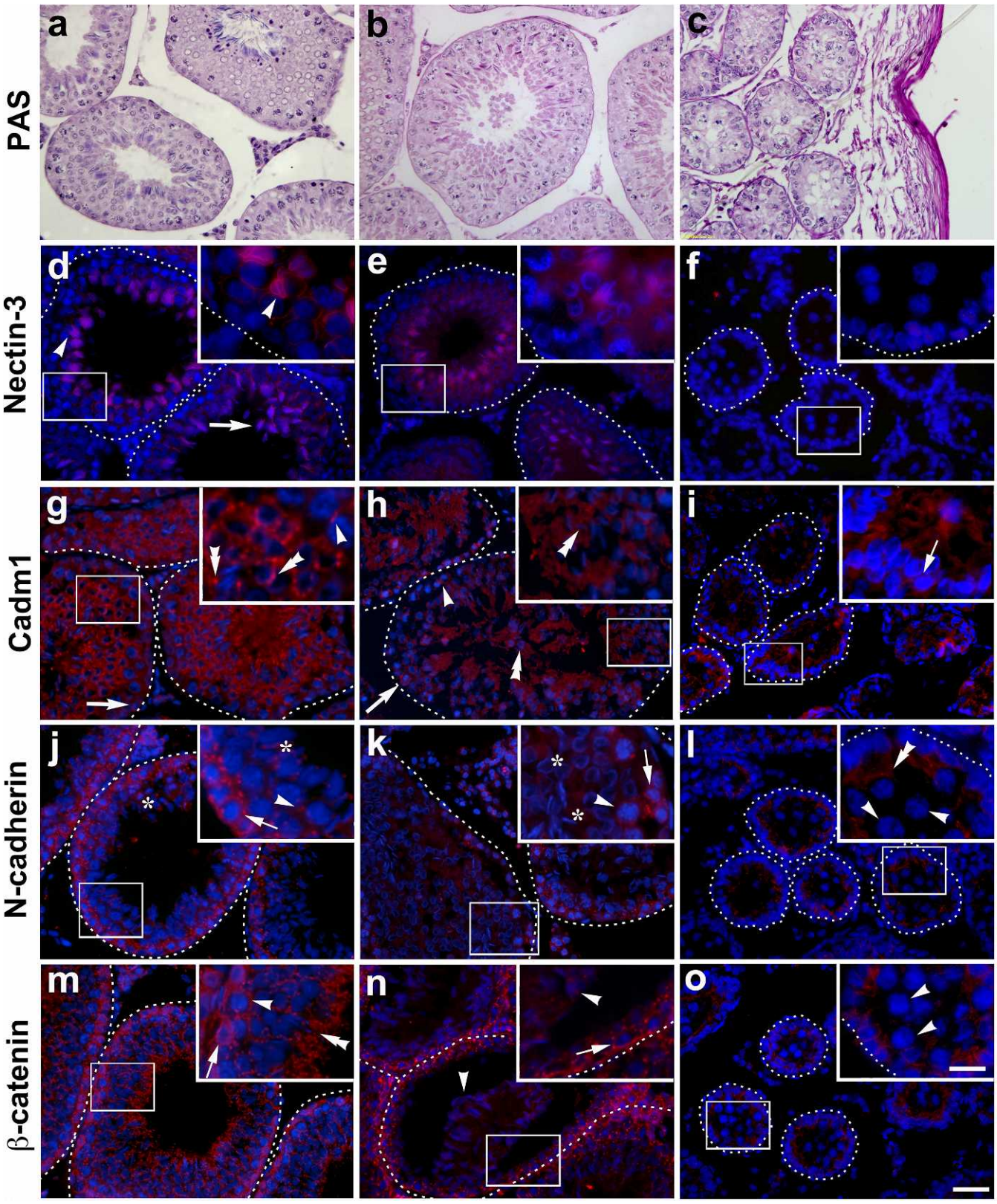

FIG. 2. Changes in the immunolocalization pattern of nectin-3 (**d**–**f**), Cadm1 (**g**–**i**), N-cadherin (**j**–**l**), and β-catenin (**m**–**o**) during spermatogenesis regression. Histological sections (PAS stained) of active (**a**), phase I (**b**), and advanced phase III (**c**) testes. **d**) Arrowheads, elongating spermatid; arrows, tip of the acrosomes. **g**) Arrow, spermatogonium; arrowhead, spermatocytes; double arrowheads, round and elongating spermatids. **h**) Arrow, spermatogonium; arrowhead, spermatocytes; double arrowheads, round and elongating spermatids. **i**) Arrow, spermatogonium. **j**) Arrow, spermatogonium; arrowhead, spermatocytes; asterisk, round and elongating spermatids. **k**) Arrow, spermatogonium; arrowhead, spermatocyte; asterisk, elongating spermatid. **l**) Double arrowhead, Sertoli cell domains; arrowheads, spermatocytes. **m**) Arrow, spermatogonium; arrowhead, spermatocyte; double arrowhead, elongating spermatids. **n**) Arrow, spermatogonium; arrowheads, elongating spermatids. **o**) Arrowheads, spermatocytes. Bar = 50 μm; inset bar = 20 μm.

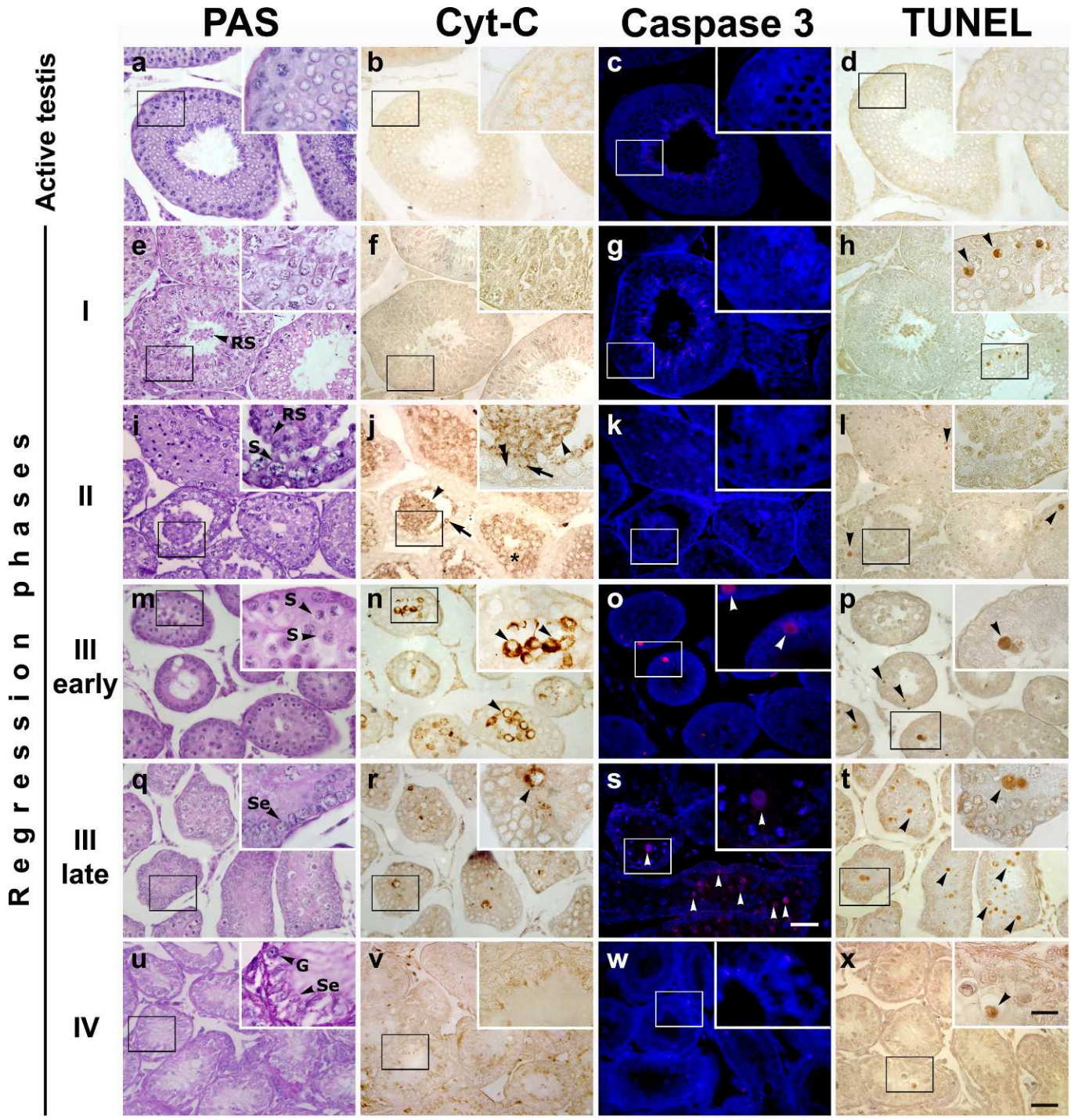

FIG. 3. Localization of apoptotic markers in individuals with active spermatogenesis or during the four phases of regression. Seminiferous tubules (PAS stained) of testes of individuals with active (**a**) or regressing (**e**, **i**, **m**, **q**, and **u**) spermatogenesis. **b**, **f**, **j**, **n**, **r**, and **v**) Cyt-C. **c**, **g**, **k**, **o**, **s**, and **w**) Caspase 3. **d**, **h**, **l**, **p**, **t**, and **x**) TUNEL. **j**) Arrowheads and arrows, spermatids; asterisks and double arrowhead, spermatocytes. **n**, **r**, **o**, **s**, **h**, **l**, **p**, **t**, and **x**) Arrowheads, spermatocytes. Se, Sertoli cell; G, spermatogonium; S, spermatocyte; RS, round spermatid. Bar = 50 μm; inset bar = 20 μm.

with PAS, underwent immunodetection for cytochrome *c* or caspase 3, or were analyzed using the TUNEL assay. In individuals with active spermatogenesis (Fig. 3a), the number of apoptotic cells was extremely low; in an entire testis cross section containing about 800 transverse tubules, only 10–15 cells showed positivity for any of the markers used [3]. Figure 3, b–d is an example of a typical tubule cross section without detectable apoptotic cells. We observed similar patterns in animals with testis activity at phase I of regression (Fig. 3e), with the exception of a few TUNEL-positive ($TUNEL^{+}$) cells (Fig. 3h) detected in 7.00% ± 1.41% of the seminiferous tubules. Interestingly, these latter cells were spermatocytes, whereas the group of postmeiotic cells detached from the epithelium and present in the lumen was TUNEL negative ($TUNEL^{-}$). In the seminiferous epithelium undergoing phase II regression (Fig. 3i), the most striking feature was that postmeiotic cells, either shed into the lumen (Fig. 3j, arrowhead) or not (Fig. 3j, arrow), were positive for

cytochrome *c* (Cyt-C$^+$) but negative for both caspase (caspase 3$^-$) and TUNEL (Fig. 3, k and l). Interestingly, spermatocytes were negative (Fig. 3j, double arrowhead) for the three apoptotic markers during exfoliation of the postmeiotic cells, but they became Cyt-C$^+$ (Fig. 3j, asterisk) when tubules were completely depleted of spermatids. The number of TUNEL$^+$ spermatocytes remained very low (about one to three per tubule cross section; Fig. 3l, arrowhead), but the frequency of tubules with positive cells increased up to 64.00% ± 5.35%. In inactive phase III specimens (Fig. 3, m and q), most spermatocytes had a strong Cyt-C$^+$ signal (Fig. 3n), whereas only a few were caspase 3$^+$ (Fig. 3o) or TUNEL$^+$ (Fig. 3p); the frequency of tubules with TUNEL$^+$ cells increased up to 72.75% ± 2.06%. In a more advanced phase III (Fig. 3q), the remaining spermatocytes were positive to all markers of apoptosis in 100% of tubules (Fig. 3, r–t), which was most evident with the TUNEL assay, in which the number of positive cells per tubule greatly increased (Fig. 3t, arrowheads) compared with previous phases of regression. In phase IV (Fig. 3u), characterized by the almost complete absence of meiotic cells, the very few remaining spermatocytes showed only the late TUNEL apoptotic marker (Fig. 3x, arrowhead).

Sertoli Cell Phagocytic Activity Contributes to the Regression of the Seminiferous Epithelium

In active testes (Fig. 4, a–c), Sertoli cells showed typical ultrastructural features, similar to those of nonseasonal species, with few small lipid droplets (Fig. 4a, asterisks), simple lysosomes (Fig. 4a, lines), no evidence of phagosomes, and many intermediate vimentin filaments associated with the desmosome-like intercellular junctions between Sertoli cells (Fig. 4b, arrows) and between Sertoli cells and germ cells (Fig. 4c, arrows). These Sertoli cell features changed in inactive testes (Fig. 4, d–f). Lipid droplets were abundant in the cytoplasm (Fig. 4d, asterisks), and phagosomes (Fig. 4d, arrowheads) appeared as complex, large bodies engulfing lipid droplets, vesicles, and organelle remains. In the adluminal compartment, desmosome-like junctions appeared with few or no intermediate vimentin filaments (Fig. 4d, inset). Overall, in Sertoli cells the intermediate filaments were severely diminished in quantity. On the other hand, the intercellular junctions between Sertoli cells and Sertoli and germ cells remained intact near the basal compartment (Fig. 4, e and f). The basement membrane was thickened with indentations (Fig. 4d, double-ended arrow), confirming its shape changes seen in light microscopy (Fig. 1e). The phagocytic activity of Sertoli cells also was demonstrated by the disappearance of germ cells, which were replaced with empty, large vacuoles located at the lumen of the seminiferous tubules (Fig. 4g, asterisks). Meiotic and postmeiotic germ cells were degenerated at variable degrees depending on the advancement of the nonbreeding season. Spermatocytes had deformed shape and contracted nuclei, and the cytoplasm was filled with vesicles (Fig. 4g, lines), whereas normal organelles were absent. However, at least at the beginning of the inactive season, spermatocyte nuclei conserved synaptonemal complexes (Fig. 4g, arrowhead) and the chromatin did not appear compact, as it did in apoptotic cells. Basal spermatogonia had a normal appearance, and near the end of the inactive season they divided mitotically to restart the regeneration of the germinal epithelium (Fig. 4h). In the interstitial tissue, numerous mast cells were present (Fig. 4i), and Leydig cells showed a higher quantity of lipid droplets in their cytoplasm (Fig. 4j, asterisks).

Together, these morphological features describe an alteration of the functional activity of the seminiferous epithelium that encompasses degeneration of germ cells (with the exception of spermatogonia) and indicates, at advanced stages of testis regression, phagocytic activity of Sertoli cells. However, this alteration does not seem to affect the intercellular junctions at the basal compartment (Fig. 4, e and f). Interestingly, in the interstitial compartment, a reduction of the interstitial cell activity is accompanied by the presence of mastocytes.

DISCUSSION

Germ cell loss is the main cause of seminiferous epithelium regression in many mammalian seasonal breeders [3–10]. Importantly, in the large hairy armadillo, this process occurs very rapidly during a period of about 2 wk [3], when we observe, as a consequence of cell detachment and death, progressive alterations to the histological organization of the seminiferous epithelium. Concomitant with cell detachment is an increased diffusion of the immunosignals that localize the molecules involved in the interaction between germ cells and between Sertoli cells and germ cells (i.e., nectin-3, Cadm1, N-cadherin, and β-catenin), an indication of a stepwise loss of cell-to-cell interaction. For nectin-3, this specific role was demonstrated in the mouse when anti-nectin-3 antibodies were injected within the lumen of the seminiferous epithelium. The presence of the antibodies led to the disruption (with the involvement of nectin-2 and Afidin) of the actin filaments at the Sertoli cell-maturing spermatid ectoplasmic specializations, and to the subsequent detachment of maturing spermatids [14]. Likewise, knockout mice for Cadm1 show shedding of spermatocytes and spermatids from the seminiferous epithelium [15], highlighting the crucial functional role of this molecule in the maintenance of the tissue architecture.

The signal/s and mechanisms of spermatogenesis regression in seasonal breeders leading to germ cell loss are poorly understood. The 12-fold decrease in the level of gonad testosterone that we measured in animals with phase IV seminiferous epithelium [3] is likely to play a crucial role, as has also been shown in a number of other seasonal breeders [4, 5, 10] or after experimental testosterone withdrawal [18, 19]. Similarly to our findings, in the inactive testis of the seasonal breeder Iberian mole, β-catenin, E-cadherin, and N-cadherin antibodies display a homogeneously diffused staining throughout the epithelium layers [10]. Furthermore, in rats, experimental intratesticular androgen suppression leads to the dissociation of N-cadherin from β-catenin at the interface between Sertoli cell-spermatid interface (adluminal compartment) and Sertoli-Sertoli cell interface (basal compartment). The concurrent diffusion of these molecules occurs at the initial phase of epithelium regression and likely reflects a loss of protein-to-protein association [20]. Both studies demonstrate that alterations of the adherens junctions and of the ectoplasmic specializations located at the Sertoli cell-germ cell contact areas end with the sloughing of germ cells in advanced meiotic and postmeiotic stages of differentiation.

In the present study we highlight the cytoskeleton of Sertoli cells as a novel and crucial player in the process of germ cell regression. The cytoskeleton of mammalian Sertoli cells contains three types of elements—actin filaments, vimentin intermediate filaments (a characteristic of these cells), and microtubules—that have different functions during spermatogenesis [21]. Whereas microtubules and actin filaments are involved in sperm release, intermediate filaments have scarcely been investigated. They are located at the perinuclear space, from where they radiate towards the cell periphery and associate with the desmosome-like junctions between Sertoli-

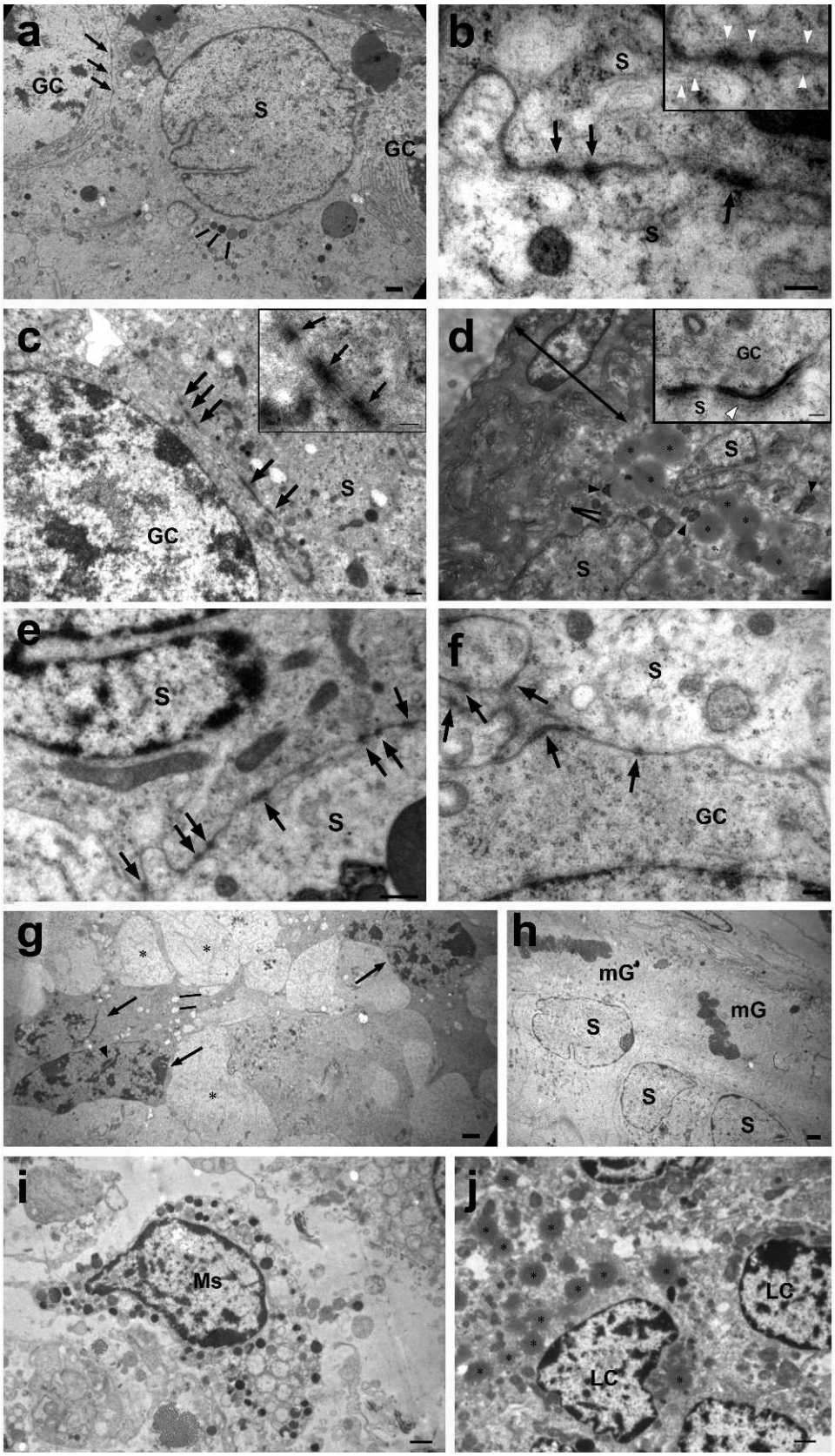

FIG. 4. Ultrastructural features of active and inactive testes. The fine structure of Sertoli cells (S) in the active testis (**a**–**c**) has normal appearance, with only a few lipid droplets (asterisks) and lysosomes (lines) in the cytoplasm (**a**), and many intermediate filaments of vimentin (**b**, inset, white arrowheads) associated with the desmosomelike (arrows) intercellular junctions between Sertoli cells (**b**) and Sertoli-germ cells (**a** and **c**, GC). In regressing testis (**d**–**j**), although these intercellular junctions can also be observed near the basal compartment (compare arrows in **b** and **c** with those in **e** and **f**), the cytoplasm of Sertoli cells shows radical changes, such as an increase in lipid droplets (**d**, asterisks), phagosomes (**d**, arrowheads), and lysosomes (**d**, lines), and a very large decrease in intermediate filaments (**d**, inset, white arrowhead; GC, primary spermatocyte); an increase in the thickness of the tubular wall (**d**, double

Sertoli and Sertoli-germ cells [21, 22]. Although their function remains mostly unknown, their association with desmosomes at the intercellular junctions between Sertoli cells and germ cells suggests their possible involvement in the maintenance of the upper layers of the seminiferous epithelium. During the breeding season, the vimentin filaments are organized as bundles surrounding the nucleus and radiating to the cell periphery, where they are associated with the desmosome-like junctions. When we looked at the intercellular spaces in the adluminal compartment of the inactive epithelium, the dense plates corresponding to desmosome-like junctions were still visible, but the bundles of vimentin filaments on the Sertoli side of the junctions were not seen, except for a few cases that presented only one or two individual filaments. Similar detrimental effects were described when testosterone levels were experimentally reduced, resulting in the cleavage and fragmentation of the vimentin intermediate filaments but leaving the actin microfilaments or the microtubules unaltered [19]. The subsequent loss of branching of these filaments from the perinuclear location towards the lumen and the desmosomelike junctions causes an alteration of the function of the adherens cell junctions.

In summary, our results suggest a loss of adhesion between Sertoli cells and both meiotic and postmeiotic cells in a process of exfoliation of the spermatids, which almost completely fill the lumen, followed by the detachment of spermatocytes and the collapse of the seminiferous tubules. This loss of adhesion involves nectin-3, Cadm1, N-cadherin, and β-catenin, together with a dramatic reduction in the extension of the vimentin filaments associated with desmosome-like junctions at the interface between Sertoli and germ cells in the adluminal compartment, thus indicating a possible relationship between these changes and the detachment of the germ cells. With regression progressing, germ cells detach from Sertoli cells, which at this stage lack junctions. These findings are novel and add new players to the mechanisms involved in the process of seminiferous epithelium regression occurring in seasonal breeders. In *C. villosus*, these mechanisms do not involve the disassembly of the Sertoli-Sertoli cell junctions associated with the establishment of the blood-testis barrier (BTB), consistent with the androgen suppression model in the rat [20]. At this stage, our results do not give evidence of the integrity of the BTB, an issue that will be addressed in future experiments using functional in vivo assays. The armadillo may be different from the Iberian mole, in which, after completion of germ cell desquamation, full testis regression entails the disassembly of the BTB [10].

There is debate over the actual role of apoptosis in the regression of mammalian spermatogenesis once germ cells are detached [10]. As summarized in Figure 5, our results indicate that the late apoptotic TUNEL marker is insufficient to explain the massive cell loss occurring at phases I and II, because it evidences very few positive cells. Instead, the immunocytochemical pattern of the early marker cytochrome *c* clearly speaks in favor of an apoptotic pathway of cell elimination, a pathway that is active in phase III, as shown by the positivity to the three apoptotic markers and by TEM analysis, which revealed signs of cell degeneration.

We propose that germ cell apoptosis is triggered by the cells' detachment from Sertoli cells, resembling a particular type of cell death named anoikis. In its classical definition anoikis occurs in epithelial tissues as a consequence of the disruption of cell-matrix interactions [23], whereas in the seminiferous epithelium, following testosterone withdrawal, it is rather a consequence of loss of adhesion between Sertoli and germ cells [24]. Although we did not use hallmarks of anoikis, such as Bmf [24], the simultaneous loss of Sertoli-germ cell adhesion and the release of cytochrome *c* from mitochondria speak in favor of this particular type of cell death, which is different from the process of live germ cell desquamation that occurs without apoptosis in the Iberian mole [10]. Postmeiotic cells were positive for cytochrome *c* but were negative for the late apoptotic markers caspase 3 and TUNEL (phase II) and completely disappeared from the seminiferous epithelium at phase III of regression, suggesting their elimination before the occurrence of the late phase of apoptosis. At this stage, we do not know where and how these cells are eliminated. A hypothesis is that they may reach the epididymis; however, although our histological analysis did not give evidence of their presence in this trait, we cannot exclude their presence in sections more proximal to the testis. Unfortunately, no epididymal tissue from the single animal in phase II regression is currently available to allow recognition of postmeiotic cell morphology or to allow immunohistochemical analysis using either meiotic, postmeiotic, or apoptotic markers. In addition, we may not exclude that sloughed postmeiotic cells undergoing apoptosis might be phagocytosed by Sertoli cells, as has been experimentally proven by the injection of apoptotic germ cells into the seminiferous tubules of mice treated with busulfan for the depletion of both meiotic and postmeiotic germ cells [25].

At advanced stages of regression (phases III–IV), the few spermatocytes that remained were positive for both early (cytochrome *c*) and late (caspase 3 and TUNEL) apoptotic markers, a sign that in these germ cells this molecular cascade was completed. At these stages of regression (phases III–IV), the cytoplasmic engulfment of cell debris and of lipid droplets within Sertoli cells indicates their phagocytic activity. Our observations are corroborated by previous electron microscopy studies where Sertoli cells phagocytized degenerating germ cells (Russell and Clermont [26], Chemes [27], Nakanishi and Shiratsuchi [28], and Wang et al. [29], and references therein).

The physiological regression of testis activity does not solely affect the seminiferous epithelium, but also implies changes of the interstitial tissue, such as alterations to the cytoplasm of Leydig cells—including a greater number of lipid droplets—and the increased number of mastocytes in the interstitium (J.P. Luaces, unpublished results).

Overall, the results of our study together with previous knowledge indicate a sequence of events that is critical to the process of seminiferous epithelium regression in mammalian seasonal breeders and underline aspects that are specific to the armadillo. In *C. villosus*, we envisage the following scenario: first, the 12-fold decrease in the testosterone levels recorded during the inactive period [3] triggers a cascade of events that, as a consequence, disrupts the adhesion apparatus at the interface between Sertoli and germ cells. Then, two subsequent events of germ cell loss occur that involve an initial exfoliation

arrow); degenerating spermatocytes (**g**, arrows); abnormalities of the interstitial tissue as well as the presence of many mast cells (**i**, Ms) and an increment of lipid droplets (**j**, asterisks) in the cytoplasm of Leydig cells (**j**, LC). Synaptonemal complexes (**g**, arrowhead); small vesicles in the cytoplasm of the spermatocytes (**g**, lines); large vacuoles near the lumen (**g**, asterisks); and mG, spermatogonia in mitosis (**h**), are shown. Bar = 1 μm (**a**, **d**, **i**, and **j**), 0.5 μm (**c** and **e**), 2 μm (**g** and **h**), 0.2 μm (**b** and **f**), and 100 μm (insets).

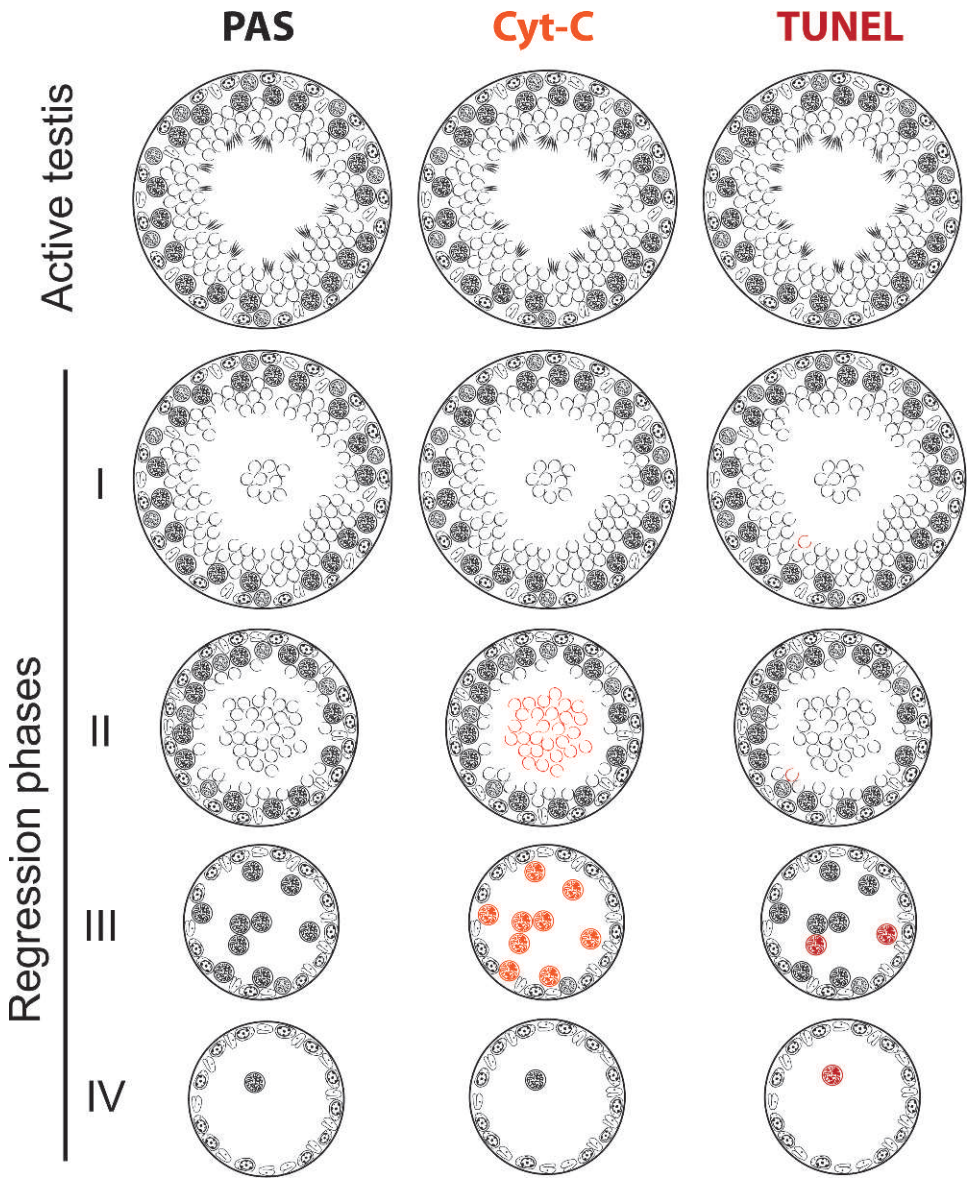

FIG. 5. Graphical representation of the localization of apoptotic markers during the four phases of seminiferous epithelium regression.

of the postmeiotic cells and later the apoptosis of the meiotic layer. Once released into the lumen of the tubule, postmeiotic cells initiate apoptosis and are rapidly eliminated by an as yet unknown process before its completion. Instead, residual meiotic cells go through all of the stages of apoptosis and are then eliminated by the Sertoli cells.

Here we report for the first time how testis regression takes place in a species of the Southern Hemisphere mammalian clade, the xenarthrans, one of the earliest offshoots among placentals [30]. Our results, together with other Xenarthra characteristic reproductive features [2, 3], provide evidence that substantial physiological differences may account for the existence of different mechanisms of testis regression in mammals.

Finally, the large hairy armadillo, with its rapid arrest and subsequent reacquisition of full spermatogenic activity, is coming out as a novel model in reproductive biology.

REFERENCES

1. Wetzel RM. Taxonomy and distribution of armadillos, Dasypodidae. In: Montgomery GG (ed.), The Evolution and Ecology of Armadillos, Sloths and Vermilinguas. Washington, DC, and London: Smithsonian Institution Press; 1985:23–56.
2. Luaces JP, Ciuccio M, Rossi LF, Faletti AG, Cetica PD, Casanave EB, Merani MS. Seasonal changes in ovarian steroid hormone concentrations in the large hairy armadillo (*Chaetophractus villosus*) and the crying armadillo (*Chaetophractus vellerosus*). Theriogenology 2011; 75(5): 796–802.
3. Luaces JP, Rossi LF, Merico V, Zuccotti M, Redi CA, Solari AJ, Merani, MS, Garagna S. Spermatogenesis is seasonal in the large hairy armadillo, *Chaetophractus villosus* (Dasypodidae, Xenarthra, Mammalia). Reprod Fertil Dev 2012; 25:547–557.
4. Furuta I, Porkka-Heiskanen T, Scarbrough K, Tapanainen J, Turek FW, Hsueh AJ. Photoperiod regulates testis cell apoptosis in Djungarian hamsters. Biol Reprod 1994; 51:1315–1321.
5. Morales E, Pastor LM, Ferrer C, Zuasti A, Pallares J, Horn R, Calvo A, Santamaría L, Canteras M. Proliferation and apoptosis in the seminiferous epithelium of photoinhibited Syrian hamsters (*Mesocricetus auratus*). Int J Androl 2002; 25:281–287.
6. Young KA, Nelson RJ. Mediation of seasonal testicular regression by apoptosis. Reproduction 2001; 122:677–685.
7. Strbenc M, Fazarinc G, Bavdek SV, Pogacnik A. Apoptosis and proliferation during seasonal testis regression in the brown hare (*Lepus europaeus* L.). Anat Histol Embryol 2003; 32:48–53.

8. Blottner S, Schön J, Roelants H. Apoptosis is not the cause of seasonal testicular involution in roe deer. Cell Tissue Res 2007; 327:615–624.
9. Dadhich RK, Real FM, Zurita F, Barrionuevo FJ, Burgos M, Jiménez R. Role of apoptosis and cell proliferation in the testicular dynamics of seasonal breeding mammals: a study in the Iberian mole, *Talpa occidentalis*. Biol Reprod 2010; 83(1):83–91.
10. Dadhich RK, Barrionuevo FJ, Real FM, Lupiañez DG, Ortega E, Burgos M, Jiménez R. Identification of live germ-cell desquamation as a major mechanism of seasonal testis regression in mammals: a study in the Iberian mole (*Talpa occidentalis*). Biol Reprod 2013; 88(4):101.
11. Shi SR, Chaiwun B, Young L, Cote RJ, Taylor CR. Antigen retrieval technique utilizing citrate buffer or urea solution for immunohistochemical demonstration of androgen receptor in formalin-fixed paraffin sections. J Histochem Cytochem 1993; 41(11):1599–1604.
12. Cetica PD, Sassaroli J, Merani MS, Solari AJ. Comparative spermatology in Dasypodidae (*Priodontes maximus*, *Chaetophractus villosus* and *Dasypus hybridus*). Biocell 1993; 18:89–103.
13. Cetica PD, Solari AJ, Merani MS, De Rosas JC, Burgos MH. Evolutionary sperm morphology and morphometry in armadillos. J Submicrosc Cytol Pathol 1998; 30:309–314.
14. Toyama Y, Suzuki-Toyota F, Maekawa M, Ito C, Toshimori K. Disruption of ectoplasmic specializations between Sertoli cells and maturing spermatids by anti-nectin-2 and anti-nectin-3 antibodies. Asian J Androl 2008; 10(4):577–584.
15. Wakayama T, Iseki S. Role of the spermatogenic–Sertoli cell interaction through cell adhesion molecule-1 (Cadm1) in spermatogenesis. Anat Sci Int 2009; 84(3):112–121.
16. Johnson KJ, Boekelheide K. Dynamic testicular adhesion junctions are immunologically unique. II. Localization of classic cadherins in rat testis. Biol Reprod 2002; 66(4):992–1000.
17. Chang Y-F, Lee-Chang JS, Harris KY, Sinha-Hikim AP, Rao MK. Role of β-catenin in post-meiotic male germ cell differentiation. PLoS ONE 2011; 6(11):e28039.
18. O'Donnell L, McLachlan RI, Wreford NG, De Kretser DM, Robertson DM. Testosterone withdrawal promotes stage-specific detachment of round spermatids from the rat seminiferous epithelium. Biol Reprod 1996; 55(4):895–901.
19. Show MD, Anway MD, Folmer JS, Zirkin BR. Reduced intratesticular testosterone concentration alters the polymerization state of the Sertoli cell intermediate filament cytoskeleton by degradation of vimentin. Endocrinology 2003; 144:5530–5536.
20. Xia W, Wong CH, Lee NP, Lee WM, Cheng CY. Disruption of Sertoli-germ cell adhesion function in the seminiferous epithelium of the rat testis can be limited to adherens junctions without affecting the blood–testis barrier integrity: an in vivo study using an androgen suppression model. J Cell Physiol 2005; 205(1):141–157.
21. Vogl AW, Vaid KS, Guttman JA. The Sertoli cell cytoskeleton. Adv Exp Med Biol 2008; 636:186–211.
22. Aümuller G, Schulze C, Viebahn C. Intermediate filaments in Sertoli cells. Microsc Res Tech 1992; 20:50–72.
23. Frisch SM, Francis H. Disruption of epithelial cell-matrix interactions induces apoptosis. J Cell Biol 1994; 124:619–626.
24. Show MD, Folmer JS, Anway MD, Zirkin BR. Testicular expression and distribution of the rat bcl2 modifying factor in response to reduced intratesticular testosterone. Biol Reprod 2004; 70(4):1153–1161.
25. Nakagawa A, Shiratsuchi A, Tsuda K, Nakanishi Y. In vivo analysis of phagocytosis of apoptotic cells by testicular Sertoli cells. Mol Reprod Dev 2005; 71(2):166–177.
26. Russell LD, Clermont Y. Degeneration of germ cells in normal, hypophysectomized and hormone treated hypophysectomized rats. Anat Rec 1977; 187(3):347–365.
27. Chemes H. The phagocytic function of Sertoli cells: a morphological, biochemical, and endocrinological study of lysosomes and acid phosphatase localization in the rat testis. Endocrinology 1986; 119:1673–1681.
28. Nakanishi Y, Shiratsuchi A. Phagocytic removal of apoptotic spermatogenic cells by Sertoli cells: mechanisms and consequences. Biol Pharm Bull 2004; 27(1):13–16.
29. Wang H, Wang H, Xiong W, Chen Y, Ma Q, Ma J, Ge Y, Han D. Evaluation on the phagocytosis of apoptotic spermatogenic cells by Sertoli cells in vitro through detecting lipid droplet formation by Oil Red O staining. Reproduction 2006; 132(3):485–492.
30. Asher RJ, Bennett N, Lehmann T. The new framework for understanding placental mammal evolution. Bioessays 2009; 31(8):853–864.